DOI: 10.1002/cmdc.200600300

Fluorescent Probes for Rapid Screening of Potential Drug–Drug Interactions at the CYP3A4 Level

Antoinette Chougnet,[a] Yelena Grinkova,[b] David Ricard,[a] Stephen Sligar,[b] and Wolf-D. Woggon*[a]

Steroid derivatives bearing fluorescent groups such as anthracene, dansyl, deazaflavin, and pyrene attached to C6 were synthesized. These compounds are unique inhibitors of cytochrome P450 3A4 (CYP3A4) and display similar IC_{50} values in the μM range for the CYP3A4 substrates midazolam, testosterone, and nifedipine. On binding to CYP3A4, the fluorescence of the dansyl, deazaflavin, and pyrene probes is quenched by photophysical interaction of the fluorophore with the heme. The addition of drug candidates with binding constants in the nM–μM range causes displacement of the probes from the active site, and hence leads to restoration of fluorescence. Accordingly, relative affinities of drug candidates to CYP3A4 can be easily and accurately determined by fluorescence measurements.

Introduction

Cytochrome P450 3A4 (CYP3A4), a heme–thiolate protein, is one of the most abundant P450 enzymes in the human liver.[1] The ability of CYP3A4 to metabolize more than 50% of therapeutic agents explains the large number of documented drug–drug interactions associated with CYP3A4 induction or inhibition.[2–4] It is therefore of great importance to measure the affinity of new drug candidates toward CYP3A4 as early as possible to determine their potential as inhibitors and to evaluate their influence on the metabolism of co-administered drugs.

Some particular features of the active site of CYP3A4 make this goal difficult to achieve. First, several distinct binding sites (at least three) have been described using testosterone (**1**), midazolam (**2**), and nifedipine (**3**) as substrates (Figure 1).[5] Furthermore, it has been shown that more than one substrate molecule can bind simultaneously to the enzyme.[6–8] Partial inhibition and even activation have been observed when a pair of drugs was co-incubated.[9,10] Finally, X-ray crystallographic structures of truncated forms of CYP3A4, a membrane-bound enzyme, have become available only recently.[8,11,12] These data may allow the development of an in silico model to evaluate the affinity of drugs for CYP3A4, but this approach is still under investigation.[13]

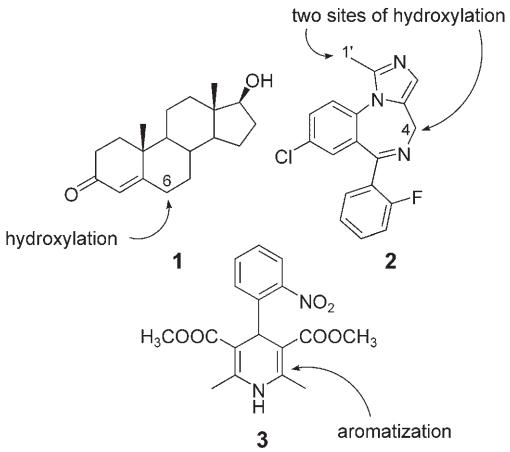

Figure 1. Cytochrome P450 3A4 substrates used for inhibition studies.

Our aim was to develop a probe that blocks the different binding sites of CYP3A4 such that the affinity of drug candidates could be evaluated by its displacement in a single assay, without performing tedious enzyme inhibition studies with several substrates. The design of our probes has been guided by the following considerations: first, we thought it would be an advantage to evaluate the affinity of the parent compound or drug *exclusively* in the absence of any metabolism. One of the inconveniences of classical methods with standard substrates such as **1**, **2**, or **3** is indeed that a catalytically competent enzymatic system is required.[14] During incubation, the compound to be tested may also be metabolized, leading to a complex mixture with time-dependent composition containing several compounds with different affinities to CYP3A4. Second, it would be advantageous to use a fluorescence method for

[a] *Prof. Dr. A. Chougnet, Dr. D. Ricard, Prof. Dr. W.-D. Woggon*
Department of Chemistry, University of Basel
St. Johanns-Ring 19, 4056 Basel (Switzerland)
Fax: (+41) 61-267-11-02
E-mail: wolf-d.woggon@unibas.ch

[b] *Y. Grinkova, Prof. Dr. S. Sligar*
Department of Biochemistry, University of Illinois
505 South Goodwin Ave., Urbana, IL 61801 (USA)

Supporting information for this article is available on the WWW under http://www.chemmedchem.org or from the author.

the determination of CYP3A4 affinities, because this analysis is highly sensitive and easily adaptable to high-throughput screening tests. Finally, the probe should block the different sites of CYP3A4 simultaneously to avoid problems related to the possible binding of new drug candidates to several sites of CYP3A4.

In this context it is interesting to note that nifedipine (**3**), for example, inhibits the metabolism of testosterone (**1**) but testosterone does not inhibit the CYP3A4-catalyzed oxidation of nifedipine.[5] From this observation we concluded that both **1** and **3** bind to the active site of CYP3A4, and **3** forms a π–π interaction with the heme chromophore preventing access of the steroid to the oxo iron(IV) porphyrin radical cation (CpdI). This hypothesis was an important part of the design of inhibitor **4**, in which testosterone is substituted at C6 with a flexible linker terminated with a fluorophore such as deazaflavin. The proposed binding mode of **4** with CYP3A4 heme is shown as complex **5** (Figure 2).

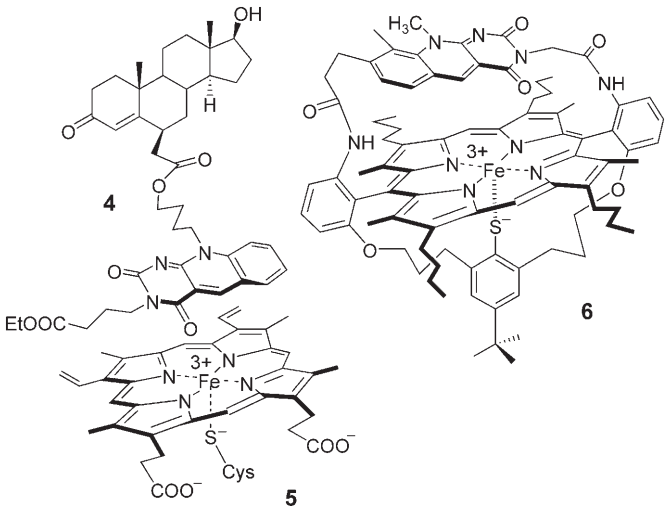

Figure 2. Complex **5**: proposed interaction of **4** with the heme of CYP3A4; the synthetic model system **6** was used for investigation of the photophysical interaction between deazaflavin and the iron(III)-containing porphyrin.[15]

In this construct the putative binding sites of the steroid are maintained, the site of hydroxylation is occupied, and the deazaflavin unit that takes the stacking role of nifedipine permits photophysical interaction with the iron porphyrin. Using a synthetic model system **6** which mimics this interaction we have recently shown that the fluorescence of the deazaflavin moiety is quenched mainly through intersystem crossing (ISC) processes supported by the paramagnetic iron(III).[15] Furthermore, the combination of two different binding modes as in **5** is expected to produce an affinity higher than for each isolated subunit, restricting the flexibility of the CYP3A4 active site and hence preventing the access of other molecules.

Herein we report the synthesis of several steroid derivatives substituted with different fluorescent moieties from which the deazaflavinyl testosterone derivative **4** seems to be the most promising fluorescent probe for detecting potential drug–drug interactions at the CYP3A4 level.

Results and Discussion

Syntheses of steroid derivatives

The steroid units **7**, **8**, and **9** were all prepared from the parent compounds **1** and **1a** by nucleophilic addition to the corresponding π-allyl Pd complexes **10**, **11**, and **12** followed by hydrolysis and subsequent decarboxylation. Published procedures were used for these sequences[16,17] (Scheme 1). The steroids substituted in position 6β were obtained as major isomers; the amount of the 6α epimer was generally below 5%

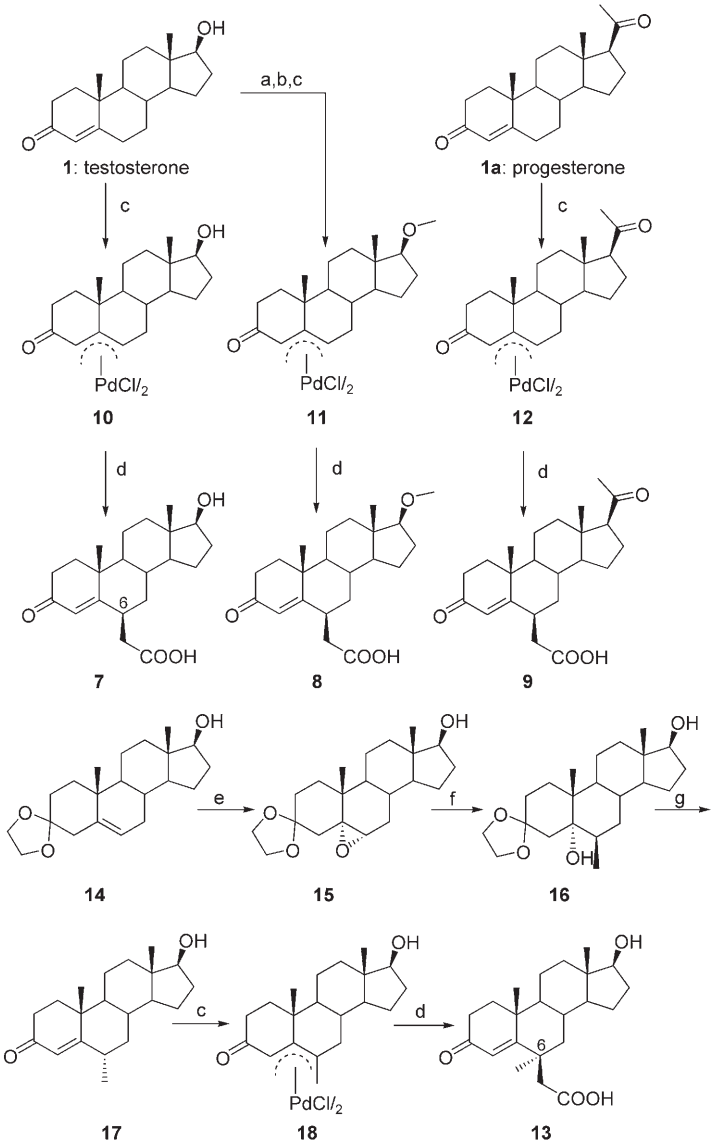

Scheme 1. Synthesis of steroid derivatives: a) ethylene glycol, *p*TsOH, benzene; b) 1) NaH, ICH_3, THF, 2) $HClO_4$, THF; c) $PdCl_2$, NaCl, THF; d) 1) NaH, dimethylmalonate, DMSO, 2) LiI, DMF, 3) LiOH, MeOH/H_2O; e) *m*-chloroperbenzoic acid, $NaHCO_3$, CH_2Cl_2; f) CH_3MgCl, THF; g) 1) $HClO_4$, THF, 2) KOH, MeOH, 3) *p*TsOH, THF. DMF = *N*,*N*-dimethylformamide, DMSO = dimethylsulfoxide, Ts = toluenesulfonyl.

with careful control of the decarboxylation and final ester hydrolysis.

The testosterone derivative **13**, doubly substituted at C6, was prepared to prevent any possible epimerization. Compound **13** was synthesized from the ketal of testosterone **14** starting with a sequence involving stereospecific epoxidation leading to **15**, followed by regio- and stereospecific Grignard ring opening to **16**. Subsequent deprotection and epimerization at C6 furnished 6α-methyltestosterone **17**,[18] which was converted into the α-configured π-allyl Pd complex **18**. Nucleophilic β attack of the dimethyl malonate anion and subsequent decarboxylation and saponification yielded the desired **13**.

The steroids were then ready to be coupled with four fluorophores that were selected owing to their well-documented fluorescence properties[19,20] and which were expected to display a π–π stacking interaction with the cofactor of CYP3A4. The anthracenyl, dansyl, and pyrenyl units **19**, **20**, and **21** are commercially available, and **20** and **21** were derivatized to obtain the alcohols **22**[21] and **23**.[22] The deazaflavinyl alcohol **24** was synthesized from 6-chlorouracil **25**[23,24] in three steps via **26** and **27** (Scheme 2).

The desired CYP3A4 fluorescence probes **4** and **28**–**33** (Figure 3) were then obtained by coupling the alcohols **24**, **19**, **22**, and **23** with the various steroid acids **7**, **8**, **9**, and **13** in the presence of *N*-ethyl-*N*′-(3-dimethylaminopropyl)carbodiimide hydrochloride (EDC) and 4-dimethylaminopyridine (DMAP).[25] It is important to note that these reaction conditions did not lead to epimerization at C6. According to ^{1}H NMR analysis the protons at C4 of the 6α and 6β epimers are well separated by 60–70 Hz, such that the epimeric purity can be easily determined. The compounds used contained less than 5% of the 6α epimer.

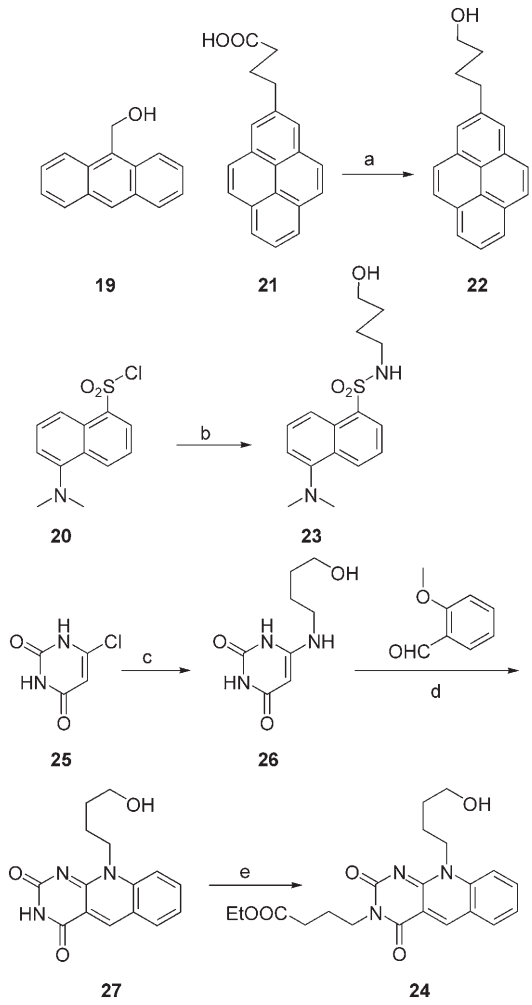

Scheme 2. Synthesis of fluorophores: a) $LiAlH_4$, THF; b) 4-aminobutanol, NEt_3, CH_2CL_2; c) 4-aminobutanol, *n*-butanol; d) 2-methoxybenzaldehyde, DMF; e) 4-bromoethylbutyrate, K_2CO_3, DMF.

Inhibition experiments

IC_{50} values of **4** and **28**–**33**, measured by incubation of substrates **1**–**3** with CYP3A4-containing microsomes,[26] were found to be rather uniform in the low-μM region (Table 1). From these studies several important facts emerged: 1) the IC_{50} values obtained with the three substrates are all of the same order of magnitude, 2) **4**, **28**, and **29** prevent oxidation at the two sites of midazolam (C1′ and C4, Figure 1), whereas published data[5b] indicate that testosterone alone inhibits C1′ hydroxylation of midazolam, but not oxidation at C4. These values show that the different probes prevent access of **1**, **2**, and **3** to their respective binding sites. IC_{50} values are generally better than those obtained for the fluorophores alone. For example, the IC_{50} values for **4** and **24** are 2.5 and 240 μM, respectively, with testosterone as substrate.[27]

The similar IC_{50} values of **4**, **32**, and **33** indicate that modifications at C17 of the steroid moiety are rather insignificant for interaction with the CYP3A4 binding site. Furthermore, the small percentage of 6α epimer present in probes **4**, **28**–**30**, and **32**–**33** is clearly not important because **31**, a single isomer with a β-configured fluorophore linker, displays IC_{50} values well within the range of the other compounds. This is also true for 6α-**4** as reported in reference [27].

Binding and displacement of fluorescence probes

As a result of the turbidity of microsome suspensions in buffer, fluorescence measurements in this system proved to be unsatisfactory. In contrast, a soluble CYP3A4 preparation from Calbiochem (3A4-Cal) or CYP3A4 incorporated into nanodiscs (3A4-nano)[6,28] gave reproducible results. In a typical experiment, **4** (1 μM final concentration) was mixed with a twofold excess of CYP3A4, irradiation at $\lambda_{ex} = 400$ nm produced λ_{em} at 480 nm.

The intensity of the latter was quenched relative to a solution of **4** lacking CYP3A4 by 80%[27] and 50% for 3A4-Cal and 3A4-nano, respectively (Figure 4A). From control experiments such as UV-difference spectroscopy (type I spectra, Figures 5 and 6) it can be estimated that the binding constant of **4** to 3A4-nano (dissociation constant of the enzyme–substrate complex: $K_d = 0.3$ μM) is very similar to that determined previously for **4** and 3A4-Cal ($K_d = 0.5$ μM).[27] Thus the difference in the

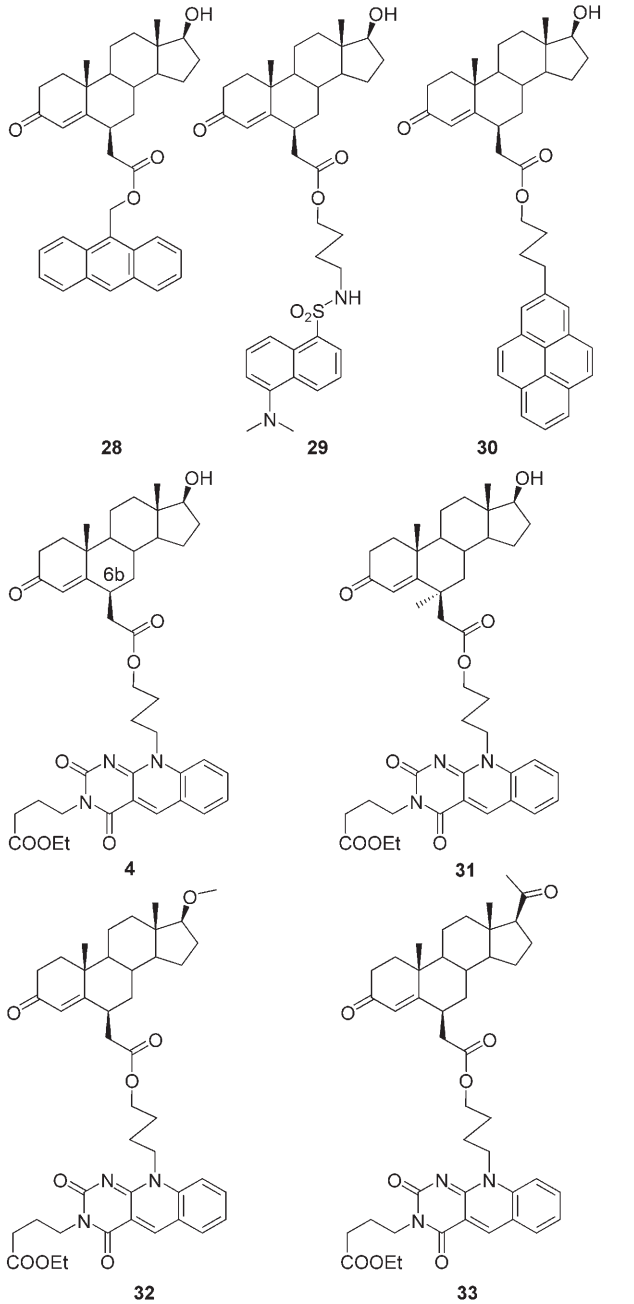

Figure 3. Structures of CYP3A4 fluorescence inhibitors; photophysical properties: **4** and **31**–**33**: $\lambda_{ex}=400$ nm, $\lambda_{em}=478$ nm; **28**: $\lambda_{ex}=365$ nm, $\lambda_{em}=412$ nm; **29**: $\lambda_{ex}=336$ nm, $\lambda_{em}=500$ nm; **30**: $\lambda_{ex}=341$ nm, $\lambda_{em}=376$ nm.

extent of quenching for the two systems is not due to differences in affinities. It may be due to distinct orientations of **4** relative to the heme within the binding pocket, the fluorescence intensities being influenced by the distance and/or angle of the emitter to the quencher.[15] It may also depend on the presence of aggregates in the solubilized enzyme 3A4-Cal.

Nevertheless, in both cases the addition of ketoconazole[29] (**34**; $K_i=50$–100 nM depending on substrate[30]) displaces inhibitor **4** from the active site of CYP3A4 and hence restores fluorescence. Figure 4 also shows the results obtained with anthracenyltestosterone **28**, dansyltestosterone **29** and pyrenotestosterone **30.** For inhibitors **29** and **30**, significant fluorescence quenching was observed when the fluorescent probes were mixed with the enzyme in a ratio of 1:2. Fluorescence can be restored by the addition of increasing amounts of ketoconazole (**34**). The fluorescence was completely restored when ketoconazole was present at a final concentration of 20 μM. The anthracenyl derivative **28** behaved quite differently: only slight fluorescence quenching was observed upon binding with CYP3A4, and the addition of ketoconazole had no significant effect. Thus it seems that for **28**, which is a good inhibitor (Table 1), the linker between the steroid and fluorophore is too short to assure an observable photophysical interaction of the anthracenyl moiety with the heme.

Table 1. IC_{50} values of various inhibitors for substrates **1**–**3**, incubation with CYP3A4 containing microsomes.[6]

Inhibitor	IC_{50} [μM] 1[a]	2[a,b]	3[a]
28	2.3 ± 0.6	0.74 ± 0.08	2.4 ± 0.6
		1.6 ± 0.5	
29	0.26 ± 0.5	0.8 ± 0.1	0.55 ± 0.5
		0.9 ± 0.1	
30	1.7 ± 1	1.1 ± 0.5	3.8 ± 1
4	2.5 ± 0.6	1.1 ± 0.5	4.1 ± 0.2
		1.0 ± 0.5	
31	1.34 ± 0.2	0.95 ± 0.10	0.54 ± 0.04
32	1.84 ± 0.14	1.2 ± 0.2	0.5 ± 0.2
33	0.71 ± 0.08	0.5 ± 0.2	0.58 ± 0.08

[a] Substrate concentrations at respective K_M values: **1**, 56 μM; **2**, 3 μM; **3**, 5 μM. [b] The first value refers to the formation of 1′-hydroxymidazolam (major metabolite), the second refers to the formation of 4-hydroxymidazolam (minor metabolite).

Using compound 4 to identify inhibitors of CYP3A4 which may cause drug–drug interactions

Detailed kinetic analyses performed with testosterone as substrate have confirmed that **4** is a competitive inhibitor of CYP3A4 with a K_i value of 1.5 μM. This probe was further used for ranking different compounds by their relative affinity for CYP3A4. Testosterone (**1**), midazolam (**2**), mibefradil (**35**) and ketoconazole (**34**) (Figure 7) were used as surrogates of new drug candidates for testing the concept. They were added to a mixture of **4** (1 μM) and 3A4-Cal (2 μM) at different concentrations. The displacement of **4** from CYP3A4 is followed by the increase of the fluorescence signal (Figure 8).

As expected, testosterone (**1**; $K_i=380$ μM)[5] was unable to significantly restore fluorescence even at concentrations as high as 30 μM. Midazolam (**2**; $K_i=10$ μM) added at a concentration of 10 μM leads to a 10% increase in fluorescence, and at 30 μM, a 20% increase. Mibefradil (**35**) was withdrawn from the market because of drug–drug interactions observed when this drug was co-administered with statins.[31] This compound presents a high affinity for CYP3A4 ($K_i=0.6$ μM[32]). As expected, mibefradil (**35**) restored as much as 40% of the fluorescence at a concentration of 10 μM. As already mentioned, ke-

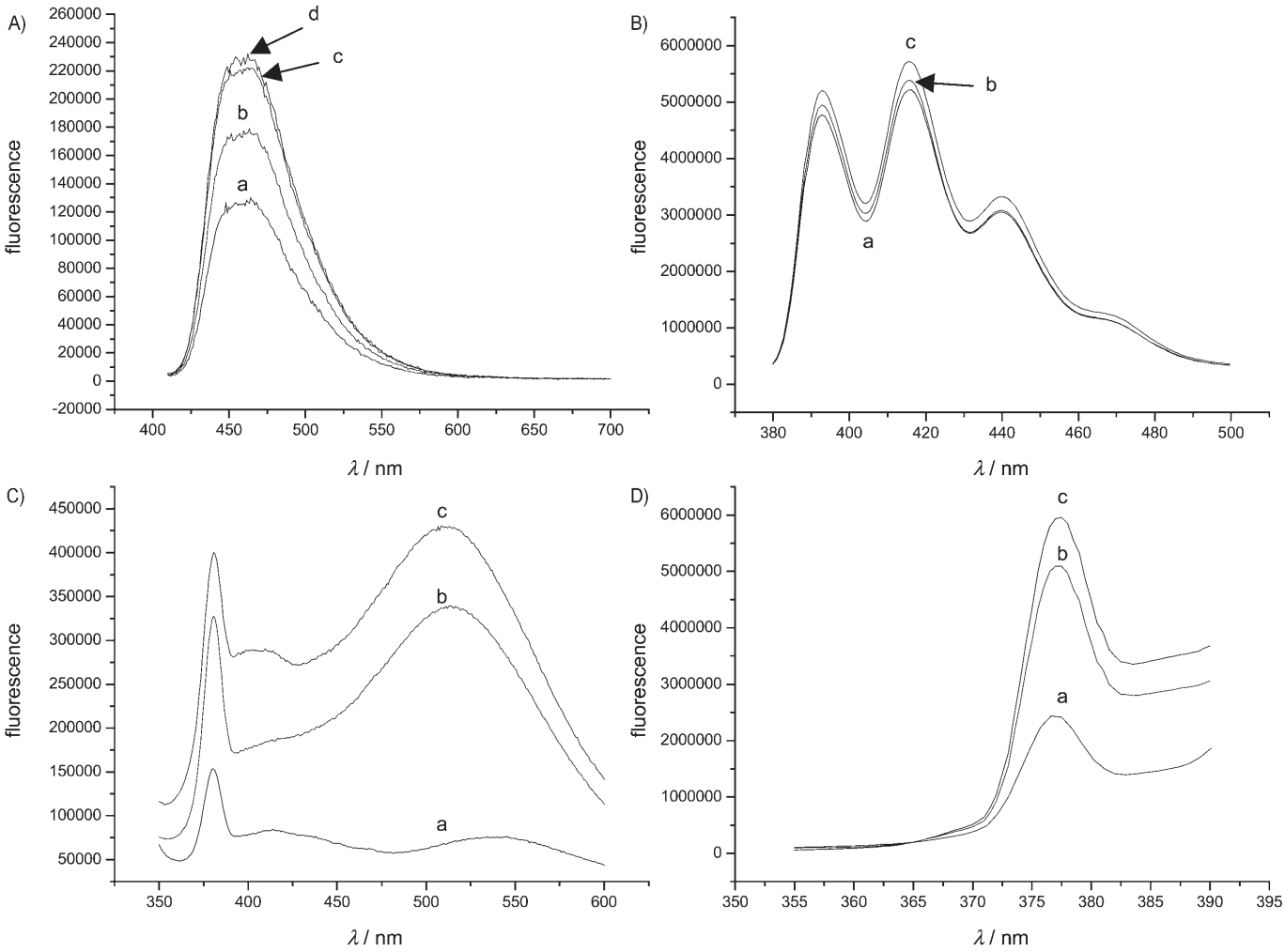

Figure 4. Binding of various steroid inhibitors to 3A4-nano and displacement by ketoconazole (**34**). A) Fluorescence emission observed by mixing deazaflavinyltestosterone **4** (1.08 μM) and 3A4-nano (1.9 μM) (a) and adding 1 μM (b), 20 μM (c), and 40 μM (d) ketoconazole. B) Fluorescence emission observed by mixing anthracenyltestosterone **28** (1 μM) and 3A4-nano (1.9 μM) (a) and adding 1 μM (b) and 20 μM (c) ketoconazole. C) Florescence emission observed by mixing dansyltestosterone **29** (1 μM) with 3A4-nano (1.9 μM) (a) and adding 1 μM (b) and 20 μM (c) ketoconazole. D) Fluorescence emission observed by mixing pyrenotestosterone **30** (1 μM) and 3A4-nano (1.9 μM) (a) and adding 1 μM (b) and 20 μM (c) ketoconazole. Addition of ketoconazole (20 μM) displaces the probes from the active site.

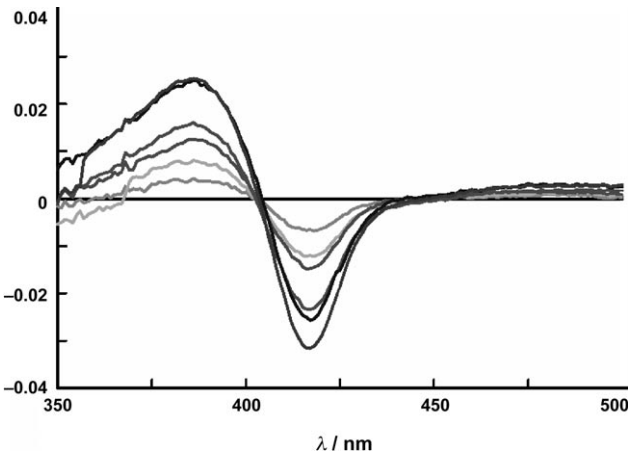

Figure 5. UV/Vis differential spectra: addition of compound **4** at 0.2, 0.4, 0.6, 1.0, 1.5, and 2.9 μM (light gray traces to black) to 3A4-nano (1.1 μM) incorporated into nanodiscs.

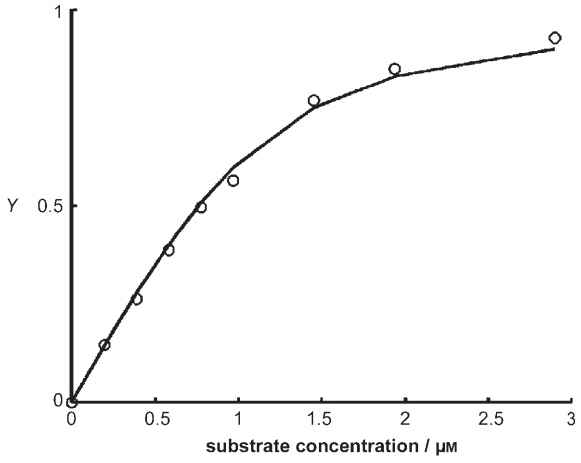

Figure 6. 3A4-nano titration data with **4** fitted with the exact equation for tight binding when the enzyme concentration (1.1 μM) is greater than K_d (0.3 μM).[33] The fraction of the enzyme with the substrate bound, *Y*, is expressed as: $Y=((E_t+S_t+K_d)-((E_t+S_t+K_d)^2-4E_tS_t)^{1/2})/(2E_t)$.

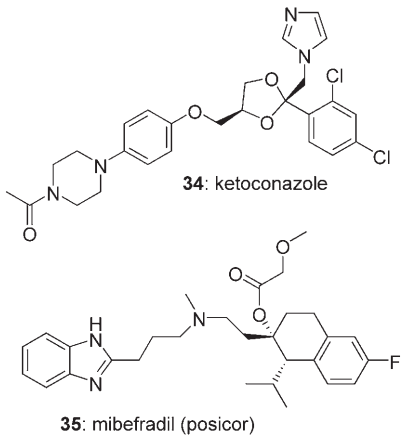

Figure 7. Structures of strong CYP3A4 inhibitors.

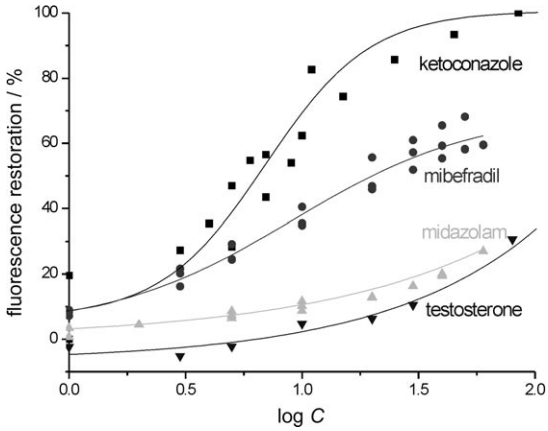

Figure 8. Displacement of **4** (1 mM) from the active site of 3A4-Cal (1.9 mM) by increasing amounts of testosterone (**1**), midazolam (**2**), ketoconazole (**34**), and mibefradil (**35**).

toconazole, one of the most potent inhibitors of CYP3A4, was able to displace more than 80% of **4** at 10 μM.

The presence of nonspecific binding may explain the unexpected high concentration necessary to displace more than 50% of the probe from the active site. Nevertheless, the effect of the four compounds tested on the fluorescence of **4** in a solution of CYP3A4 is in good agreement with their respective affinities reported in the literature.

Conclusions

In vivo drug–drug interactions have become an increasingly important issue in drug development. Some of these problems are related to CYP3A4 inhibition. Owing to the presence of several substrate binding sites, the extremely versatile metabolic enzyme CYP3A4 requires rather tedious assays with three different substrates.

The fluorescent probes described herein offer a new perspective, particularly in combination with CYP3A4 assembled into nanodiscs (3A4-nano): 1) a simple fluorescence assay allows the determination of the relative CYP3A4 affinities of new drug candidates; 2) a complete catalytic system with turnover and analysis of metabolites is not required; 3) the fluorescent probes tested display rather uniform IC_{50} values in the low-μM range which can be considered adequate to evaluate whether a given compound would potentially cause drug–drug interactions; 4) this assay can be developed toward high-throughput screening.

Experimental Section

General: Recombinant human cytochrome P450 3A4 (3A4-Cal) was purchased from Calbiochem–Merck (cat. no. 250307). The supersomes were from BD Biosciences (specific activity, testosterone hydroxylation: $\geq$200 units (mg protein)$^{-1}$. Chemicals were purchased from Fluka AG, Switzerland. Expression, purification, and incorporation of CYP3A4 into nanodiscs were performed as previously described.[6] ^{1}H and ^{13}C NMR spectra were recorded on a Bruker DPX NMR (400 MHz); MS data were recorded on a Varian VG-70-250. IR spectra were measured on a PerkinElmer FTIR 1600, and for fluorescence spectroscopy an ISA Jobin Yvon-Spex Fluoromax-2 was used.

Incubation conditions: A solution of CYP3A4 (100 μL, 100 nM, human CYP3A4 + OR + b5 "supersomes", Gentest–BD Biosciences), a substrate solution in methanol (5 μL, concentrations set at 100 K_M, 0.3 mM for midazolam, 0.5 mM for nifedipine, 5.6 mM for testosterone), the inhibitor solution in methanol (5 μL), a solution (50 μL) containing 10 mM NADP, 100 mM glucose-6-phosphate, and 50 mM $MgCl_2 \cdot 6H_2O$ in 100 mM phosphate buffer pH 7.4, and phosphate buffer (290 μL, 100 mM, pH 7.4) were mixed and warmed at 37 °C for a few minutes. The reaction was initiated by the addition of a solution of glucose-6-phosphate dehydrogenase (50 μL, 20 U mL^{-1}). After 15 min, the reaction was stopped by the addition of acetonitrile (500 μL). The mixture was centrifuged, the supernatant was evaporated in a Speed-Vac, and the pellet was dissolved in a mixture of water and methanol (1:1, 50 μL) and analyzed by HPLC using a 125–3 Supersphere RP-Select B column (Merck, Germany). The compounds were eluted with an acetonitrile/ammonium acetate buffer (50 mM, pH 4.75) gradient starting with 30% acetonitrile to 50% in 30 min. Detection was performed at $\lambda = 250$ nm. With this method, the retention times of 6β-hydroxytestosterone, testosterone, 4-hydroxymidazolam, 1′-hydroxymidazolam, midazolam, oxynifedipine, and nifedipine were, respectively, 5.6, 17.3, 10.5, 13.1, 20.5, 14.6 and 15.6 min.

Synthesis of 26: A solution of dried 6-chlorouracil **25** (400 mg, 2.73 mmol) and 4-aminobutan-1-ol (506 μL, 5.47 mmol) in *n*-butanol (16 mL) was held at reflux under argon for 24 h. The reaction mixture was allowed to cool to room temperature. The product precipitated, was filtered and washed with cold *n*-butanol (5 mL). After drying in vacuo, **26** (501 mg, 92%) was obtained as a pale-yellow solid; mp: 255–256 °C; TLC: $R_f = 0.21$ (EtOAc); IR (KBr): $\tilde{\nu} =$ 3340, 3252, 3120 (NH), 1702 cm^{-1} (CO); ^{1}H NMR ($CDCl_3$): $\delta = 10.10$ (br s, 1H, NH), 9.79 (br s, 1H, NH), 6.04 (br s, 1H, NH), 4.41 (br s, 1H, OH), 4.38 (s, 1H, H-5), 3.39 (m, 2H, CH_2, H-11), 2.98 (q, $J = 6.4$ Hz, 2H, CH_2, H-8), 1.53–1.38 ppm (m, 4H, CH_2, H-9 + H-10); ^{13}C NMR ($CDCl_3$): $\delta = 165.1$ (C6), 154.9 (C2 or C5), 151.7 (C2 or C5), 73.3 (C5), 61.3 (C11), 42.1 (C8), 30.5 (C10), 25.8 ppm (C9); MS (FAB): $m/z = 200$ (100%, $[M+H]^+$).

Synthesis of 27: A solution of **26** (491 mg, 2.46 mmol) and 2-methoxybenzaldehyde (671 mg, 4.93 mmol) in dry DMF (15 mL) was held at reflux under argon for 15 h. The reaction mixture was allowed to cool to room temperature. The precipitate formed after 48 h at 0 °C was filtered, washed with cold MeOH, and dried in va-

cuo. Compound **27** (514 mg, 73%) was obtained as a yellow powder; mp: 299–300 °C; TLC: R_f = 0.21 (EtOAc); IR (KBr): $\tilde{\nu}$ = 3424, 3163, 3034 (NR), 1701 cm^{-1} (CO); ^1H NMR (DMSO): δ = 10.09 (br s, 1H, NH), 8.89 (br s, 1H, H-5), 8.18 (d, J = 7.7 Hz, 1H, H-6), 7.95 (m, 2H, H-8 + H-9), 7.52 (m, 1H, H-7), 4.67 (br s, 2H, CH_2, H-15), 4.52 (br s, 1H, H-19), 3.46 (t, J = 6.3 Hz, 2H, CH_2, H-18), 1.74 (qt, J = 7.8 Hz, 2H, CH_2, H-17), 1.58 ppm (qt, J = 7.0 Hz, 2H, CH_2, H-16); ^{13}C NMR (DMSO): δ = 162.1 (C14), 157.1 (C13), 156.6 (C2 or C4), 141.6 (C5), 139.9 (C12), 135.8 (C8), 131.9 (C6), 124.3 (C7), 121.2 (C11), 116.6 (C9), 115.0 (C4 or C2), 60.4 (C18), 44.3 (C15), 29.4 (C17), 23.8 ppm (C16); MS (FAB): m/z = 286 (100%, $[M+H]^+$), 214 (16.9%, $[M+H]^+$).

Synthesis of 24: Ethyl-4-bromobutyrate (1.02 mL, 7.12 mmol) was added to a suspension of **27** (508 mg, 1.78 mmol) and K_2CO_3 (1.48 g, 10.7 mmol) in dry DMF (50 mL), and the reaction mixture was stirred at 60 °C for 18 h. Inorganic salts were filtered off, and the solvent was removed in vacuo. The yellow oily residue obtained was purified by flash chromatography (silica gel, CH_2Cl_2/MeOH 98:2→9:1) to afford **24** (596 mg, 84%) as a yellow fluorescent solid, which was crystallized form ethanol. mp: 153–155 °C; TLC: R_f = 0.21 (EtOAc); IR (KBr): $\tilde{\nu}$ = 3396, 3240 (NR), 1730, 1696 cm^{-1} (CO); UV/Vis λ_{max} = 228, 267, 310, 321, 379, 400, 422 nm; fluorescence properties: λ_{ex} = 400 nm, λ_{em} = 447, 470 nm; ^1H NMR (DMSO): δ = 8.87 (s, 1H, H-5), 7.89 (d, ^3J = 8.1 Hz, ^4J = 1.5 Hz, 1H + t, ^3J = 7.3 Hz, ^3J = 1.5 Hz, 1H), 7.74 (d, J = 8.8 Hz, 1H), 7.48 (t, ^3J = 7.4 Hz, ^4J = 0.8 Hz, 1H), 4.80 (br s, 2H, CH_2, H-15), 4.14–4.08 (m, 4H), 3.81 (t, J = 5.9 Hz, 2H, CH_2, H-18), 2.55 (br s, 1H, OH), 2.40 (t, J = 7.6 Hz, 2H, CH_2), 2.09–1.95 (m, 4H), 1.79 (qt, J = 6.6 Hz, 2H, CH_2, H-16), 1.24 ppm (t, J = 7.1 Hz, 3H, CH_3, H-18); ^{13}C NMR (DMSO): δ = 173.4 (CO_2Et), 162.2 (C14), 157.2 (C13), 156.3 (C2 or C4), 142.9 (C5), 140.7 (C12), 135.8 (C8), 132.2 (C6), 124.9 (C7), 122.0 (C11), 116.4 (C9), 115.5 (C4 or C2), 62.3, 60.7 (C18), 44.9 (C15), 40.9, 32.4, 29.5 (C17), 24.4, 23.8 (C16), 14.6 ppm (CH_3); MS (FAB): m/z = 400 (100%, $[M+H]^+$).

Synthesis of 23: Dansyl chloride **20** (200 mg, 0.7 mmol), 4-aminobutanol (75.7 μL, 0.81 mmol) and triethylamine (308 μL, 2.2 mmol) were dissolved in 5 mL dry CH_2Cl_2 and stirred overnight under argon in the dark at room temperature. The mixture was diluted with dichloromethane, washed with saturated ammonium chloride, then with water, dried (Na_2SO_4), concentrated, and purified by column chromatography (silica gel, CH_2Cl_2/MeOH 95:5) to yield **23** (210 mg, 90%) as a yellow oil; ^1H NMR ($CDCl_3$): δ = 8.55 (d, J = 8.3 Hz, 1H), 8.28–8.30 (d, J = 8.8 Hz, 1H), 8.23–8.25 (dd, ^3J = 8.0 Hz, ^4J = 1.3 Hz, 1H), 7.17–7.19 (d, J = 7.0 Hz, 1H), 5.12 (t, J = 6.1 Hz, 1H), 2.89 ppm (s, 6H); ^{13}C NMR ($CDCl_3$): δ = 135.1, 130.7, 130.2, 130.05, 130.02, 128.7, 123.7, 119.3, 115.6, 115.2, 62.6, 45.8, 43.5, 29.8, 26.7 ppm.

General procedure for the synthesis of esters 4 and 28–33: *Preparation of* ***4***: A solution of **7** (75 mg, 0.22 mmol), **27** (86.5 mg, 0.66 mmol), DMAP (26 mg, 0.22 mmol), and EDC (62 mg, 0.33 mmol) in 2 mL dry CH_2Cl_2 was stirred overnight at room temperature under argon. The mixture was diluted with 15 mL CH_2Cl_2, washed with saturated $NaHCO_3$, water, and dried over sodium sulfate. The crude mixture was purified by column chromatography (silica gel, CH_2Cl_2/MeOH 97:3) to yield **4** (94 mg, 60%); UV/Vis ($CHCl_3$) λ_{max} = 228, 267, 310, 321, 378, 402, 423 nm; fluorescence: λ_{ex} = 400 nm, λ_{em} = 447, 470 nm. MS (FAB): m/z = 728 $[M+H]^+$; ^1H NMR ($CDCl_3$): δ = 8.86 (s, 1H), 7.86–7.95 (m, 2H), 7.63–7.65 (m, 1H), 7.47 (t, J = 7.4 Hz, 1H), 5.73 (s, 1H, H-4), 4.76 (s, 2H), 4.06–4.17 (m, 6H), 3.62 (t, J = 6.4 Hz, 1H, H-17), 2.96 (q, ^3J = 8.5 Hz, ^4J = 4.0 Hz, 1H, H-6), 2.56–2.60 (m, 1H), 2.44–2.47 (m, 1H) 2.35–2.40 (m, 4H), 1.96–2.10 (m, 4H), 1.86–1.90 (m, 6H), 1.60–1.72 (m, 5H), 1.38–1.44 (m, 2H), 1.22–1.30 (m, 7H), 1.02–1.10 (m, 1H), 0.80–0.97 (m, 3H), 0.76 ppm (s, 3H, H-18); the amount of the α epimer of **6** (5%) can be estimated from integration of the resonance of H at C4 at 5.59 ppm, d, J = 1.5 Hz, compared with the corresponding resonance of the 6β isomer (δ = 5.73 ppm, s); ^{13}C NMR ($CDCl_3$): δ = 199.8, 173.4, 171.9, 171.5, 162.2, 157.2, 156.4, 142.9, 140.5, 135.9, 132.3, 126.8, 125.0, 122.0, 116.2, 115.5, 81.8, 64.4, 60.7, 53.8, 43.2, 41.1, 40.9, 40.6, 38.7, 38.0, 36.7, 35.7, 34.4, 32.3, 31.1, 30.7, 26.4, 24.4, 23.8, 20.9, 20.6, 14.6, 11.5 ppm.

Characteristic spectroscopic data for ***31***: ^1H NMR ($CDCl_3$): δ = 8.89 (s, 1H), 7.85–7.95 (m, 2H), 7.66–7.68 (m, 1H), 7.49 (t, J = 7.4 Hz, 1H), 5.89 (s, 1H, H-4), 4.8 (s, 2H), 4.06–4.17 (m, 6H), 3.62 (m, 1H), 2.3–2.6 (m, 8H), 1.31 (s, 3H), 1.25 (t, J = 7.1 Hz, 3H), 1.22 (s, 3H), 0.81 ppm (s, 3H); ^{13}C NMR ($CDCl_3$): δ = 200.0, 173.8, 170.6, 156.8, 142.6, 140.1, 135.5, 131.9, 125.5, 124.6, 121.6, 115.8, 115.1, 81.6, 63.7, 60.4, 50.27, 45.18, 44.2, 42.7, 40.5, 39.2, 38.5, 38.3, 36.3, 33.6, 31.9, 31.1, 30.4, 28.2, 26.1, 23.33, 23.29, 21.3, 20.7, 14.2, 11.2 ppm; MS (FAB): m/z = 742.4 $[M+H]^+$.

Characteristic spectroscopic data for ***32***: ^1H NMR ($CDCl_3$): δ = 8.88 (s, 1H), 7.85–7.95 (m, 2H), 7.66–7.68 (m, 1H), 7.49 (t, J = 7.4 Hz, 1H), 5.76 (s, 1H, H-4), 4.8 (s, 2H), 4.1–4.18 (m, 6H), 3.34 (s, 3H), 3.22 (t, J = 6.4 Hz, 1H), 3.0 (m, 1H), 1.24 (m, 11H), 0.79 ppm (s, 3H); ^{13}C NMR ($CDCl_3$): δ = 199.7, 173.2, 171.8, 171.3, 161.9, 157.0, 156.2, 142.7, 140.3, 135.7, 132.1, 126.5, 124.8, 121.8, 115.9, 115.3, 90.5, 64.1, 60.5, 58.0, 53.5, 50.6, 44.4, 42.9, 40.8, 40.7, 40.3, 38.4, 37.8, 37.7, 35.4, 34.1, 32.1, 27.6, 26.2, 24.1, 23.4, 20.8, 20.4, 14.4, 11.8 ppm; MS (FAB): m/z = 742.4 $[M+H]^+$.

Characteristic spectroscopic data for ***33***: Foamy; mp: 83–85 °C; ^1H NMR ($CDCl_3$): δ = 8.94 (s, 1H), 7.94–7.90 (m, 2H), 7.66–7.68 (m, 1H), 7.50 (t, J = 7.4 Hz, 1H), 5.77 (s, 1H, H-4), 4.8 (s, 2H), 4.1–4.2 (m, 7H), 2.12 (s, 3H), 1.24 (m, 7H), 0.66 ppm (s, 3H); ^{13}C NMR ($CDCl_3$): δ = 209.2, 199.4, 173.0, 171.6, 170.8, 161.8, 156.8, 156.0, 142.6, 140.1, 135.5, 131.9, 126.5, 124.6, 121.6, 115.8, 115.1, 64.0, 63.5, 60.4, 55.8, 53.1, 44.2, 43.9, 40.7, 40.5, 40.1, 38.5, 38.2, 37.6, 35.6, 34.0, 31.9, 31.5, 30.6, 26.1, 24.4, 24.0, 23.3, 22.7, 20.9, 20.2, 14.2, 13.4 ppm; MS (FAB): m/z = 754.5 $[M+H]^+$.

Characteristic spectroscopic data for ***28***: Fluorescence: λ_{ex} = 365 nm, λ_{em} = 412 nm; ^1H NMR ($CDCl_3$): δ = 8.51 (s, 1H), 8.30–8.28 (m, 2H), 8.02–8.04 (m, 2H), 7.48–7.59 (m, 4H), 6.16 (s, 2H), 5.80 (s, 1H), 3.55 (m, 1H), 3.1 (m, 1H), 2.61–2.68 (m, 1H), 2.45–2.55 (m, 1H), 1.09 (s, 3H), 0.65 ppm (s, 3H); ^{13}C NMR ($CDCl_3$): δ = 199.5, 171.8, 170.9, 131.4, 131.0, 129.3, 129.1, 126.8, 126.4, 125.2, 123.7, 81.5, 58.9, 53.4, 50.1, 42.7, 40.6, 40.3, 38.2, 37.7, 36.2, 34.9, 34.0, 30.6, 30.3, 23.0, 20.5, 20.2, 10.9 ppm; MS (EI): m/z = 536.3 $[M]^{+\bullet}$.

Characteristic spectroscopic data for ***29***: Fluorescence: λ_{ex} = 341 nm, λ_{em} = 376 nm; ^1H NMR ($CDCl_3$): δ = 8.53 (d, J = 8.3 Hz, 1H), 8.31 (d, J = 8.8 Hz, 1H), 8.24 (dd, ^3J = 8.0 Hz, ^4J = 1.3 Hz, 1H), 7.50–7.59 (m, 2H), 7.18 (d, J = 7.0 Hz, 1H), 5.76 (s, 1H, H-4), 5.04 (t, J = 6.1 Hz, 1H), 3.89–3.99 (m, 2H), 2.89 (s, 6H), 1.25 (s, 3H), 0.80 ppm (s, 3H); ^{13}C NMR ($CDCl_3$): δ = 200.2, 171.9, 171.6, 152.4, 135.2, 130.8, 130.3, 129.9, 128.8, 126.9, 123.6, 119.2, 115.6, 81.9, 64.4, 53.8, 43.2, 43.1, 41.3, 40.6, 38.7, 38.0, 36.7, 35.9, 34.4, 31.1, 30.8, 26.8, 26.2, 23.7, 21.0, 20.6, 11.6 ppm; MS (EI): m/z = 650.2 $[M]^{+\bullet}$; MS (FAB): m/z = 651.3 $[M+H]^+$.

Characteristic spectroscopic data for ***30***: Fluorescence: λ_{ex} = 336 nm, λ_{em} = 500 nm; ^1H NMR ($CDCl_3$): δ = 8.25–7.85 (9H, pyrene), 5.76 (s, 1H, H-4), 4.16–4.22 (m, 1H), 4.04–4.10 (m, 1H), 3.55 (t, 1H), 1.14 (s, 3H), 0.67 ppm (s, 3H); ^{13}C NMR ($CDCl_3$): δ = 199.9, 172.0, 171.3, 136.6, 131.8, 131.3, 130.3, 129.0, 127.9, 127.8, 127.7, 127.1, 126.7, 126.3, 125.5, 125.4, 125.2, 125.1, 123.7, 81.9, 64.9, 53.6, 50.5, 43.1,

41.2, 40.6, 38.6, 38.0, 36.6, 35.0, 34.4, 33.4, 30.9, 29.0, 28.6, 23.6, 20.9, 20.4, 11.4 ppm; MS (EI): $m/z = 602.4$ $[M]^{+\bullet}$.

Acknowledgements

W.-D.W. and A.C. thank the Swiss National Foundation for financial support, M. Müller and C. Stoessel for technical assistance, BD Biosciences for a generous gift of CYP3A4 supersomes, and F. Hoffmann La Roche for providing midazolam, 1′- and 4-midazolam, and mibefradil. S.S. and Y.G. acknowledge support from the National Institutes of Health GM 33775.

Keywords: cytochrome P450 3A4 · drug–drug interactions · fluorescence · inhibition · porphyrins

[1] "Human Cytochrome P450 Enzymes": F. P. Guengerich in *Cytochrome P450 Structure, Mechanism and Biochemistry* (Ed.: P. R. Ortiz de Montellano), Plenum, New York, **2005**, pp. 377 – 530.
[2] J. Lilja, K. Kivisto, P. Neuvonen, *Clin. Pharmacol. Ther.* **2000**, *68*, 384 – 390.
[3] J. H. Lin, A. Y. H. Lu, *Pharmacol. Rev.* **1997**, *49*, 403 – 440.
[4] F. P. Guengerich, *Annu. Rev. Pharmacol. Toxicol.* **1999**, *39*, 1 – 17.
[5] a) R. W. Wang, D. J. Newton, N. Liu, W. M. Atkins, A. Y. H. Lu, *Drug Metab. Dispos.* **2000**, *28*, 360 – 366; b) N. A. Hosea, G. P. Miller, F. P. Guengerich, *Biochemistry* **2000**, *39*, 5929 – 5939.
[6] B. J. Baas, I. G. Denisov, S. G. Sligar, *Arch. Biochem. Biophys.* **2004**, *430*, 218 – 228.
[7] a) K. R. Korzekwa, N. Krishnamachary, M. Shou, A. Ogai, R. A. Parise, A. E. Rettie, F. J. Gonzalez, T. S. Tracy, *Biochemistry* **1998**, *37*, 4137 – 4147; b) M. J. Dabrowski, M. L. Schrag, L. C. Wienkers, W. M. Atkins, *J. Am. Chem. Soc.* **2002**, *124*, 11866 – 11867.
[8] M. Ekroos, T. Sjögren, *Proc. Natl. Acad. Sci. USA* **2006**, *103*, 13682 – 13687.
[9] F. Ueng, Y.-T. Kuwabara, Y. J. Chun, F. P. Guengerich, *Biochemistry* **1997**, *36*, 370 – 381.
[10] K. E. Kenworthy, S. E. Clarke, J. Andrews, J. B. Houston, *Drug Metab. Dispos.* **2001**, *29*, 1644 – 1651.
[11] P. A. Williams, J. Cosme, D. M. Vinkovic, A. Ward, H. Angove, P. Day, C. Vonrhein, I. J. Tickle, H. Jhoti, *Science* **2004**, *305*, 683 – 686.
[12] J. K. Yano, M. R. Wester, G. A. Schoch, K. J. Griffin, C. D. Stout, E. F. Johnson, *J. Biol. Chem.* **2004**, *279*, 38091 – 38094.
[13] M. A. Lill, M. Dobler, A. Vedani, *ChemMedChem* **2006**, *1*, 73 – 81.
[14] D. M. Stresser, A. P. Blanchard, S. D. Turner, J. C. L. Erve, A. A. Dandeneau, V. P. Miller, C. L. Crespi, *Drug Metab. Dispos.* **2000**, *28*, 1440 – 1448.
[15] M. Müller, M. Gaplovsky, J. Wirz, W.-D. Woggon, *Helv. Chim. Acta* **2006**, *89*, 2987 – 3001.
[16] D. J. Collins, W. R. Jackson, R. N. Timms, *Tetrahedron Lett.* **1976**, *17*, 495 – 496.
[17] C. D. Jones, N. R. Mason, *Steroids* **1974**, *23*, 323 – 336.
[18] J. A. Campbell, J. C. Babcok, J. A. Hogg, *J. Am. Chem. Soc.* **1958**, *80*, 4717 – 4721.
[19] R. P. Haughland, *Handbook of Fluorescent Probes and Research Chemicals*, Molecular Probes, Eugene, OR (USA), **1996**.
[20] P. Hemmerich, V. Massey, H. Fenner, *FEBS Lett.* **1977**, *84*, 5 – 21.
[21] M. Nanasawa, H. Kamogawa, *J. Polym. Sci. Polym. Chem. Ed.* **1977**, *15*, 1499 – 1502.
[22] A. Hermetter, H. Scholze, A. E. Stütz, S. G. Withers, T. M. Wrodnigg, *Bioorg. Med. Chem. Lett.* **2001**, *11*, 1339 – 1342.
[23] T. Nagamatsu, Y. Hashiguchi, F. Yoneda, *J. Chem. Soc. Perkin Trans. 1* **1984**, 561 – 565.
[24] T. Kimachi, K. Tanaka, F. Yoneda, *J. Heterocycl. Chem.* **1991**, *28*, 439 – 443.
[25] M. K. Dhaon, R. K. Olsen, K. Ramasamy, *J. Org. Chem.* **1982**, *47*, 1962 – 1965.
[26] J. T. Buters, K. R. Korzekwa, K. L. Kunze, Y. Omata, J. P. Hardwick, F. J. Gonzalez, *Drug Metab. Dispos.* **1994**, *22*, 688 – 692.
[27] A. Chougnet, C. Stoessel, W.-D. Woggon, *Bioorg. Med. Chem. Lett.* **2003**, *13*, 3643 – 3645.
[28] I. G. Denisov, Y. V. Grinkova, B. J. Baas, S. G. Sligar, *J. Biol. Chem.* **2006**, *281*, 23313 – 23318.
[29] K. E. Kenworthy, J. C. Bloomer, S. E. Clarke, J. B. Houston, *Br. J. Clin. Pharmacol.* **1999**, *48*, 716 – 727 .
[30] A. Galetin, K. Ito, D. Hallifax, J. B. Houston, *J. Pharmacol. Exp. Ther.* **2005**, *314*, 180 – 190.
[31] J. C. Krayenbühl, S. Vozeh, M. Kondo-Oestreicher, P. Dayer, *Eur. J. Clin. Pharmacol.* **1999**, *55*, 559 – 565.
[32] C. Wandel, R. B. Kim, F. P. Guengerich, A. J. J. Wood, *Drug Metab. Dispos.* **2000**, *28*, 89 – 898.
[33] I. H. Segel, *Enzyme Kinetics*, Wiley, New York, **1975**, p. 75.

Received: December 15, 2006
Revised: January 25, 2007
Published online on March 14, 2007

